Measurements and Modeling of Acoustic Scattering from Unexploded Ordnance (UXO) in Shallow Water

D.C. Calvo,[1] B.H. Houston,[1] J.A. Bucaro,[2] L. Kraus,[3] H.J. Simpson,[1] and A. Sarkissian[1]
[1]Acoustics Division
[2]Excet, Inc.
[3]Global Strategies Group

Introduction: The gradual development of coastal areas throughout the world in proximity to military training ranges and areas of past conflict has created a need to locate underwater unexploded ordnance (UXO). These ordnance, which may have veered off course and failed to detonate when they were initially released, may still pose a risk of explosion if they are subject to handling. This complicates the process of converting areas formerly restricted to military training, for instance, into areas with general undersea and surface activities such as fishing, boating, or diving. Searches for UXO can be costly and time consuming due to the large areas of water that need to be covered and the possibility that UXO are buried in the seafloor.

Probing the ocean bottom with sound waves offers an effective means of searching for UXO because sound pulses can propagate relatively long distances underwater and penetrate the seafloor. The use of low-frequency sound, which for this application is 2 to 30 kHz, has distinct advantages for this application. Sound waves in the lower end of this spectrum can easily penetrate the seafloor and inside the UXO, causing it to respond with structural acoustic scattering signatures different from other objects. This is in contrast to high-frequency sonar, which is useful for creating highly resolved images of an object lying on the ocean bottom but is less effective if the object is buried. These structural acoustic clues help in classifying whether an echo from an object corresponds to UXO or to an object that poses no risk.

We are using controlled laboratory tank experiments and computer modeling to gain a fundamental understanding of how low-frequency sound waves interact with UXO at various burial depths and in the presence of seafloor roughness. An example UXO we have examined is a 5 in. diameter rocket warhead (Fig. 1). It consists of a thick-walled steel shell with interior compartments located at its ends and an inert filler material throughout most of its body.

Measurements: The experimental geometry features a line of monopole acoustic sources that synthesizes a cylindrical wavefront that ensonifies the UXO. Both source and receiver are at a low altitude above the sand and can rotate independently about the UXO in a horizontal plane to measure the variation of scattering with incidence angle (e.g., broadside or end-on) and reception direction (e.g., backscattering or forward scattering). A measurement[1] of backscattering target
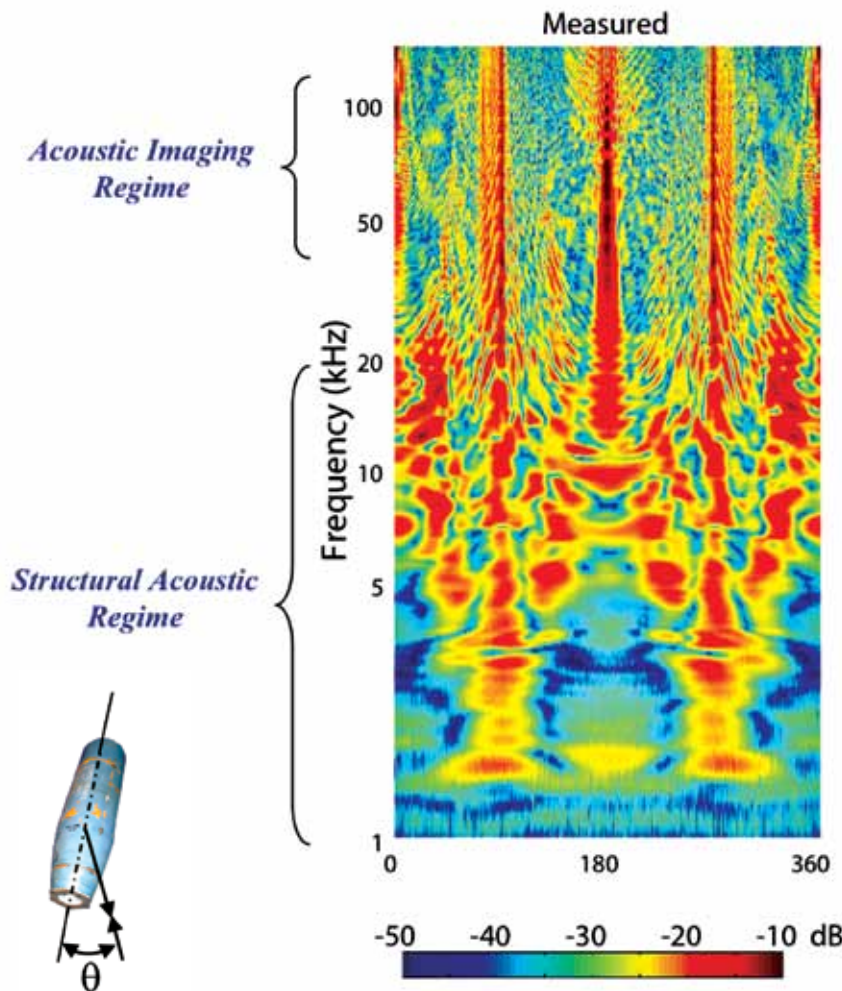

FIGURE 1
Measured backscattering target strength over a wide bandwidth of frequencies and ensonification angles for a 5-in. rocket UXO (inset) in a free-field of water.

strength as a function of frequency and incidence angle is shown in Fig. 1 for the UXO in a free-field of water (no sand is present). This figure represents a characteristic mosaic of this object that changes for objects having less internal structure or symmetry. It therefore provides clues as to whether the sonar has encountered a UXO or a less threatening object. Extensive measurements for a variety of UXO with and without sand present have been made for both monostatic[1] and bistatic[2] geometries.

Modeling: Computer modeling is helpful for interpreting phenomena seen in experiments and predicting the performance of potential search systems. Our computer modeling tools include a 2D time-domain code using the elastodynamic finite integration technique (EFIT) and a 3D finite-element code (STARS3D). To examine the limits of using a 2D model, we consider the case of broadside incidence, and model the UXO two-dimensionally by sectioning the geometry to expose a circular cross-section.

Results of using the EFIT model for a geometry used in our tank experiments are shown in Fig. 2. For this case, the UXO is located below the water-sand interface. Figures 2(a) and (b) show how the leading "head" sound pulse travels quickly through the sand and reaches the UXO first, followed by the slower arrival conveyed by the water. A comparison of arrivals at the UXO position for a flat vs a rough interface is shown in Figs. 2(b) and (c) for the same instant. Figure 2(c) illustrates how roughening the interface lengthens the bottom-penetrating pulse and increases its angular spread.

A snapshot of a scattered field, which is the difference between the pressure field with and without the UXO present, is shown in Fig. 2(d) for a flush-buried UXO. A leaky structure-borne circumferential wave persists for a considerable time that in reality depends on the amount of attenuation present. The swirling appearance is caused by the depth-dependence of the incident wave.

We also model variation in bistatic scattering in a vertical plane using the geometry depicted in Fig. 3. In addition to resonances, strong forward scattering is evident, consistent with
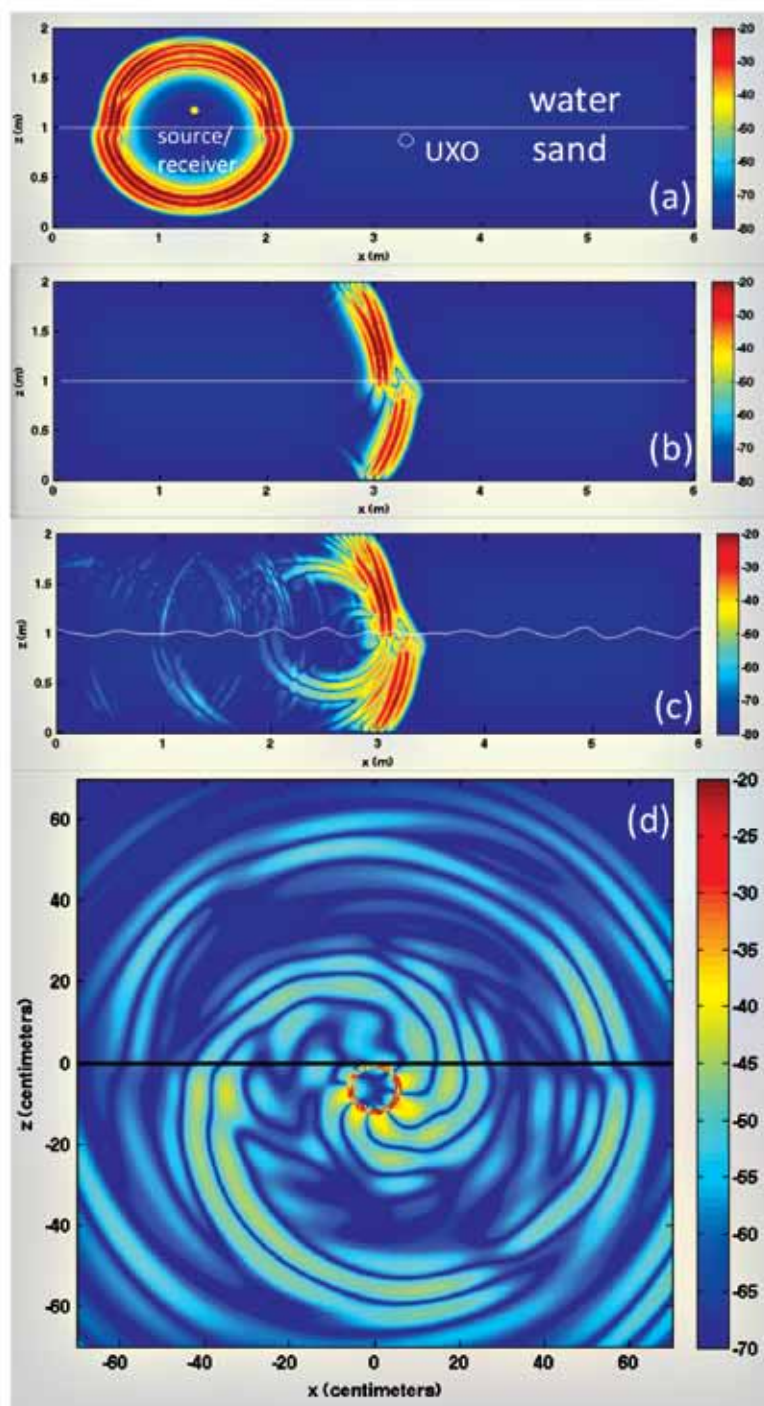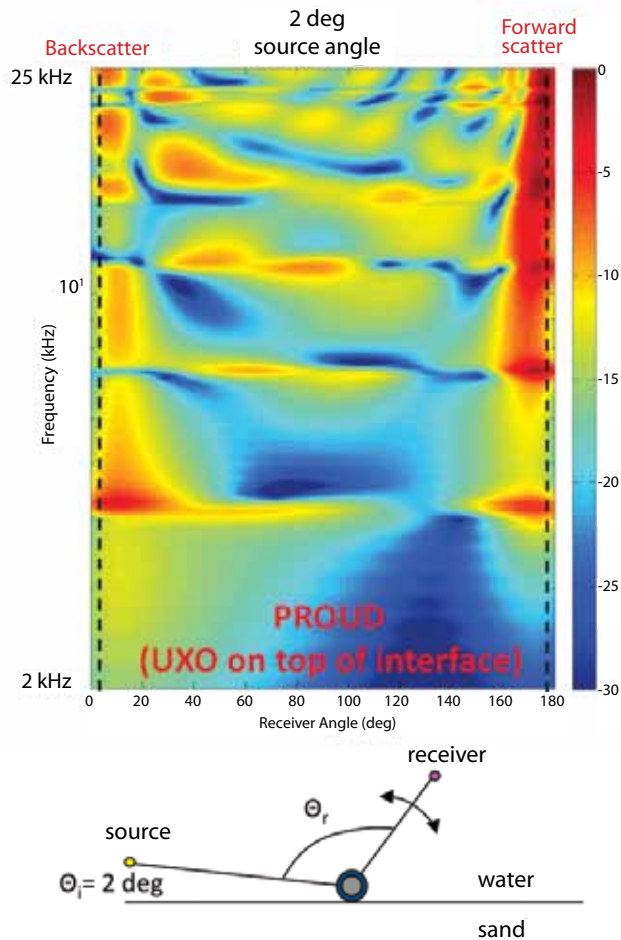

FIGURE 2
Snapshots of a computer simulation of the experiment showing the cylindrical sound pulse shortly after it has been emitted by the acoustic source (a) followed by two images (b and c) at a later instant: one with a flat and one with a roughened interface. A zoomed view of an isolated backscattered field is shown in (d) for a flush-buried UXO and a flat interface.

FIGURE 3
Simulated bistatic target strength as a function of frequency and receiver angle for scattering in a vertical plane for the 5-in. rocket UXO. Strong forward scatter is evident.

recent experimental measurements.[2] Our modeling work is also characterizing the statistical variation of the target strength as a function of sand roughness spectral parameters.[3]

Impact: This work has made the first systematic measurements of scattering from a variety of UXO in the low-frequency structural acoustics regime. The modeling efforts have shown that the essential scattering features and their dependence on burial depth can be accurately quantified. Both measurements and modeling are valuable input to object classification algorithms of potential use in UXO cleanup efforts both in the United States and throughout the world.

[Sponsored by ONR and SERDP]

References

[1] J.A. Bucaro, B.H. Houston, M. Saniga, L.R. Dragonette, T. Yoder, S. Dey, L. Kraus, and L. Carin, "Broadband Acoustic Scattering Measurements of Underwater Unexploded Ordnance (UXO)," *J. Acoust. Soc. Am.* **123**, 738–746 (2008).

[2] J.A. Bucaro, H. Simpson, L. Kraus, L.R. Dragonette, T. Yoder, and B.H. Houston, "Bistatic Scattering from Submerged Unexploded Ordnance Lying on a Sediment," *J. Acoust. Soc. Am.* **126**, 2315–2323 (2009).

[3] D. Calvo, B.H. Houston, J.A. Bucaro, L. Kraus, H. Simpson, and A. Sarkissian, "Scattering by Unexploded Ordnance (UXO) with Variable Burial Depth and Seafloor Roughness: A Parametric Study," *J. Acoust. Soc. Am.* **126**, 2167 (2009).

Scalable Wideband Frequency-Response for Free-Field, Littoral, and Seismic Applications

S. Dey[1] and W.G. Szymczak[2]
[1]GTEC, Inc.
[2]Acoustics Division

Introduction: Rapid and accurate computations of wideband frequency-domain numerical solutions are key to many structural-acoustics and seismic applications, such as acoustic radiation and scattering; automotive noise; seismic scattering; noise, vibration, and harshness (NVH) analysis; interior-noise prediction for aircrafts; and aero-acoustics.

The wave-dependent nature of such problems can lead to large dispersion errors in numerical simulation at mid-to-high frequencies unless proper discretization strategies are used. For solutions in the frequency-domain, high-order (*hp*-version) finite element approximations offer significant accuracy

advantage over low-order methods.[1] High-order, 3D discretizations for large-scale problems may contain millions of unknown solution coefficients. The solution of the resulting system of linear algebraic equations for thousands, or even hundreds, of frequencies is a significant computational effort even on parallel computing platforms.

We have developed a scalable parallel-computing scheme based on multipoint Padé approximations,[2] to accelerate the frequency-sweeping of large-scale p-finite-element approximations for wave-dependent problems. Application to 3D problems of Navy interest shows significant reduction in computational effort.

Modeling Approach: To obtain the time-harmonic response, we model the structural-acoustics problem in the frequency-domain. The elastic domain is treated as a 3D linear (visco)elastic material whose dynamic response is governed by the Navier equations of elasticity. The linear-acoustic response of the fluid domain satisfies the Helmholtz equation. For littoral applications, we treat the sediment (bottom) as a damped acoustic fluid. We solve a fully coupled system of equations with appropriate compatibility conditions at the fluid-elastic interface requiring the continuity of the normal stress and pressure and that of the normal particle acceleration. We handle the infinite extent of the exterior domain by using the so-called perfectly matched layer (PML) technique.

We use a p-finite-element discretization method resulting in a frequency-dependent system of linear algebraic equations. For a wideband frequency sweep, for N discrete circular-frequencies given by $\{\omega_1, \omega_2, ..., \omega_N\}$, we need the solutions of systems represented by the following equation:

$$A(\omega_i)u_i = b(\omega_i),\qquad(1)$$

where A and b are the frequency-dependent coefficient matrix and the right-hand-side vector, respectively, and u represents the unknown solution coefficients. We use a generalized multipoint Padé-based reconstruction that requires u and

$$\frac{d^k u}{d\omega^k}, k = 1, 2, ..., K$$

at a few coarse frequencies $\{\omega_1^0, \omega_2^0, ..., \omega_M^0\}$ with $M \ll N$. Once the coarse frequency solutions and their K derivatives with respect to frequency are known, the solution at any frequency may be reconstructed as

$$u(\omega^0 + \delta\omega) \approx \sum_{l=0}^{l=L} p_l(\delta\omega)^l / \sum_{m=0}^{m=M} q_m(\delta\omega)^m.\qquad(2)$$

Here $K = \lceil (L + M + 1)/p_n \rceil$ depends on the degree of numerator and denominator of the Padé approximation and p_n is the number of coarse frequencies used in the reconstruction. K is typically less than or equal to 10.

Taking k-successive derivatives of Eq. (1) with respect to ω and rearranging the terms gives

$$A u^{(k)} = b^{(k)} - \sum_{j=0}^{k-1} \binom{k}{j} A^{(k-j)} u^{(j)},\qquad(3)$$

where the superscript within brackets is the degree of the derivative. One can immediately note that the solution of $u^{(k)}$ is simply the solution of k additional right-hand sides for the original system matrix. Equation (3) implies that there is no cost of additional matrix factoring beyond that needed to solve the regular system.

Application and Results: Figure 4 shows the reconstruction of the bistatic scattering response for a spherical elastic shell for 256 frequencies using just three coarse frequencies. In both cases, $L = 9$, $M = 10$. This problem has 70,616 complex-valued unknown coefficients. The total time to compute the direct response for 256 frequencies in serial is 70,439 seconds. The reconstruction for using two and three coarse frequencies (one processor per coarse frequency) is 219 and 277 seconds, respectively. This implies a speedup of 321 and 254 using two and three processors, respectively.

Figure 5 depicts a cut through the 3D finite element mesh for scattering from a fully buried elastic shell. Figure 6 compares the reconstruction of the backscattering response using two, four, and eight coarse frequency points for a band of 512 frequencies. One can observe the convergence of the Padé-based reconstruction to the direct computation of the frequency-response by solving for all the frequencies. The reconstructed result using eight coarse frequency points is virtually indistinguishable for the direct response computation. The computational cost of the reconstruction-based approach, in this example, is less than the direct computation by a factor of 64.

The presented examples demonstrate the effectiveness of the approach in producing huge computational savings while preserving the accuracy of the reconstructed responses for large-scale structural acoustics.

References
[1] S. Dey and D.K. Datta, "A Parallel *hp*-FEM Infrastructure for Three-dimensional Structural Acoustics," *International Journal for Numerical Methods in Engineering* **68**(5), 583–603 (2006).
[2] P. Avery, C. Farhat, and G. Reese, "Fast Frequency Sweep Computations Using a Multi-point Padé-based Reconstruction Method and an Efficient Iterative Solver," *International Journal for Numerical Methods in Engineering* **69**(12), 2848–2875 (2007).
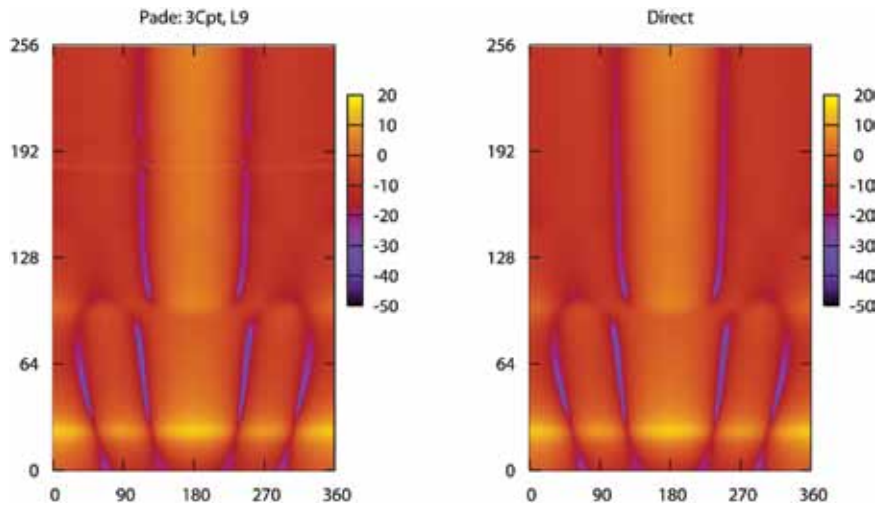
FIGURE 4
Padé-based reconstruction of bistatic-scattering response for a spherical shell (left) in free-field compared to direct computation (right).
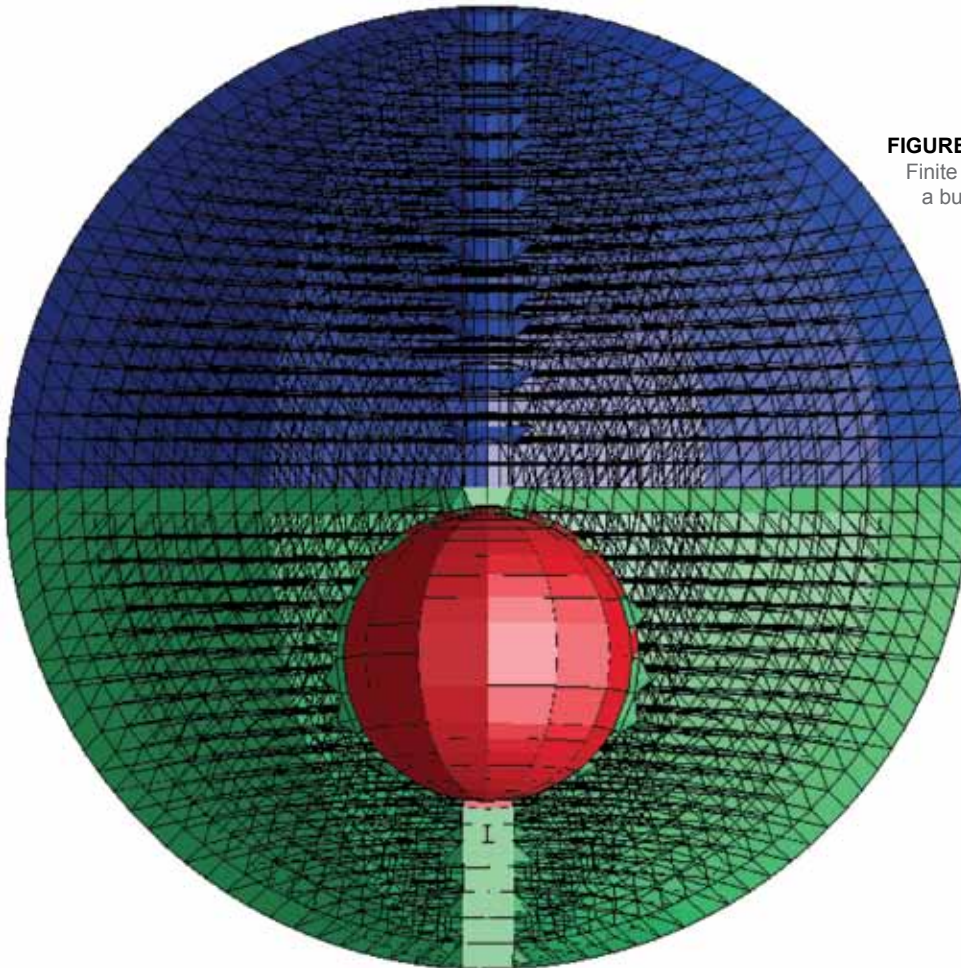

FIGURE 5
Finite element model for scattering from a buried elastic target.

FIGURE 6
Convergence of the Padé-based of the scattering response for the finite element model shown in Fig. 5.